

*Full Length Research Paper*

# Evidence of fractures from the image of the subsurface in the Akonolinga-Ayos area (Cameroon) by combining the Classical and the Bostick approaches in the interpretation of audio-magnetotelluric data

A. Meying<sup>1</sup>, T. Ndougsa-Mbarga<sup>2\*</sup> and E. Manguelle-Dicoum<sup>1</sup>

<sup>1</sup>Departement of Physics, Faculty of Science, University of Yaoundé I, P. O. Box 812 Yaoundé, Cameroon.

<sup>2</sup>Departement of Physics, Advanced Teachers' Training College, University of Yaoundé I, P. O. Box 47 Yaoundé Cameroon.

Accepted 24 September, 2009

Exploitation of audio-magnetotelluric data has been realised by combining the classical and Bostick approaches with the objective to determine the structuring of layers in the Akonolinga-Ayos subsurface area. The work has been devoted to the processing and interpretation of audio-magnetotelluric data of two profiles respectively Akonolinga-Mengueme and Mbang-Metol which are approximately running N-S and have nine stations of measurement each over a distance of 35 - 40 km. These two profiles cover a length of 70 km in the E-W direction. Different representations of data have been used and have shown interesting results. The geoelectrical sections derived from these two approaches show the topography of the subsurface with many discontinuities. This topography presents a major deep-seated fault passing through Ngultangan and Olembe and another between Ebale and Envong which passes through Awo'o, both directed E-W. Different geological sections have also been proposed. A discussion of results issued from these two approaches show that the Bostick approach brings out more details in the structuring of layers than the classical approach. The combination of the two approaches is necessary for a better interpretation of audio-magnetotelluric data as we have realized during this study.

**Key words:** Audio-magnetotelluric soundings, classical and Bostick approaches, interpretation, fault.

## INTRODUCTION

Some recent geological studies (Nzenti et al., 1988; Rolin; 1995, Toteu et al., 2004) have stated that: (1) the Congo Craton is overlapping the granulitic series of Yaoundé of the Panafrican Mobile belt and (2) the transition area between the Congo Craton/ Panafrican Mobile belt seems to be characterized by a fault which is composed of recurrent faulting. The differentiation of the Precambrian plateau and the North of Appalachians plateau in Northern America, based on the changing of the resistivity (Kurtz and Garland, 1976) and the identification of two major tectonic provinces in West Africa (Senegal) from a magnetotelluric (MT) study (Ritz, 1982), has permitted the authors to initiate the present preliminary study. The objective of this work is to observe

the behaviour of the electrical conductivity of the subsurface in the Congo Craton/Mobile Zone transition in the Akonolinga-Ayos area.

An audio-magnetotelluric (AMT) prospecting and the exploitation of data collected along two profiles having 9 sounding stations each (Figure 1c) based on the Bostick and classical approaches have permitted us to image the subsurface of the Akonolinga-Ayos region. The region under study (Figures 1a and b) is situated on the northern border of the Congo Craton in Cameroon between the latitudes 3°30'N and the 4°30'N and the longitudes 12°E and 13°15'E.

## GEOGRAPHICAL AND GEOLOGICAL SETTING

The Akonolinga-Ayos area belongs to the Congo Craton. It is located between latitudes 3°30'N and 4°30' N and

\*Corresponding author. E -mail: [tndougsa@yahoo.fr](mailto:tndougsa@yahoo.fr).

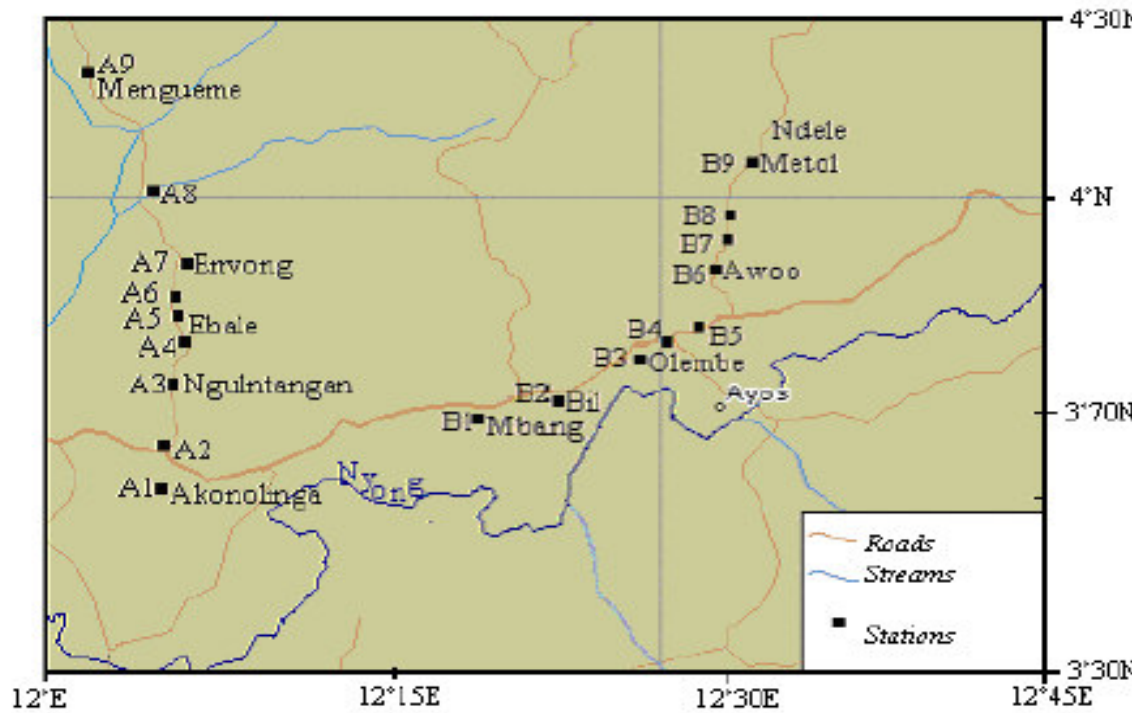


Figure 1c. Localization map of sounding stations.

longitudes 12°E and 13°15'E. The area under study (Figures 1a and b) presents an equatorial type climate and the temperatures are relatively high with an annual average of 24,64°C. The topography varies slightly with an average altitude ranging between 600 to 700 m. The area is crossed by the Nyong stream and its affluents; the Longo and the Mfoumou Rivers. A thick forest is covering 90% of the surface area of study. The flooded forest and the watery meadows are along the Nyong stream and its affluents.

A greater part of Cameroon is made up of a Precambrian basement including magmatic and metamorphic rocks belonging to different geological periods. These rocks are composed of granite and migmatite renovated during the Pan African episode. In the Akonolinga-Ayos area, the principal structural units are the Ayos series and the garnetiferous series primarily made up of quartzites, schists and micaschists (Figures 1a and b).

According to the tectonic point of view, the area of study is characterized by a transpressive senestre evolution controlled by great setbacks, N170°E of the Center of Cameroon (Olinga et al., 2009). From geological observations (Olinga et al., 2009) many structures directed E-W presenting moderated dip have been identified. These structures are probably linked to tectonics napes with a southern vergency (Vignès-Adler et al., 1991; Penaye et al., 1993; Olinga et al., 2009). The tectonic evolution of the area includes four principal phases:

- A  $D_1$  phase of deformation of unknown kinematics, marked by a foliation strongly transposed by the later deformations;
- A  $D_2$  phase comprising two progressive sequences, an initial  $D_{2a}$  sequence and a late  $D_{2b}$  sequence;
- A  $D_3$  phase of deformation characterized by large regional folds of axis N-S affecting all the former structures;
- A  $D_4$  phase of deformation materialized by normal diaclasses and faults marked by discontinuous joints clogged and not by granitic seams as usual (Olinga et al., 2009).

The geological observations based on rock lithology on one hand and tectonic facts on the other hand show the complexity of the Akonolinga-Ayos area.

## METHODOLOGY AND EQUIPMENT

### Magneto telluric method

The principles of the magnetotelluric (MT) method (Cagniard, 1953) establish that the ratio of the electric and magnetic field components,  $E_x$  and  $H_y$  respectively depend only on the frequency. This makes it possible to determine the variations of the resistivity with the depth. The fundamental equation of Cagniard is as follows:

$$\rho = 0.2T \left| \frac{E_x}{H_y} \right|^2 \quad (1)$$

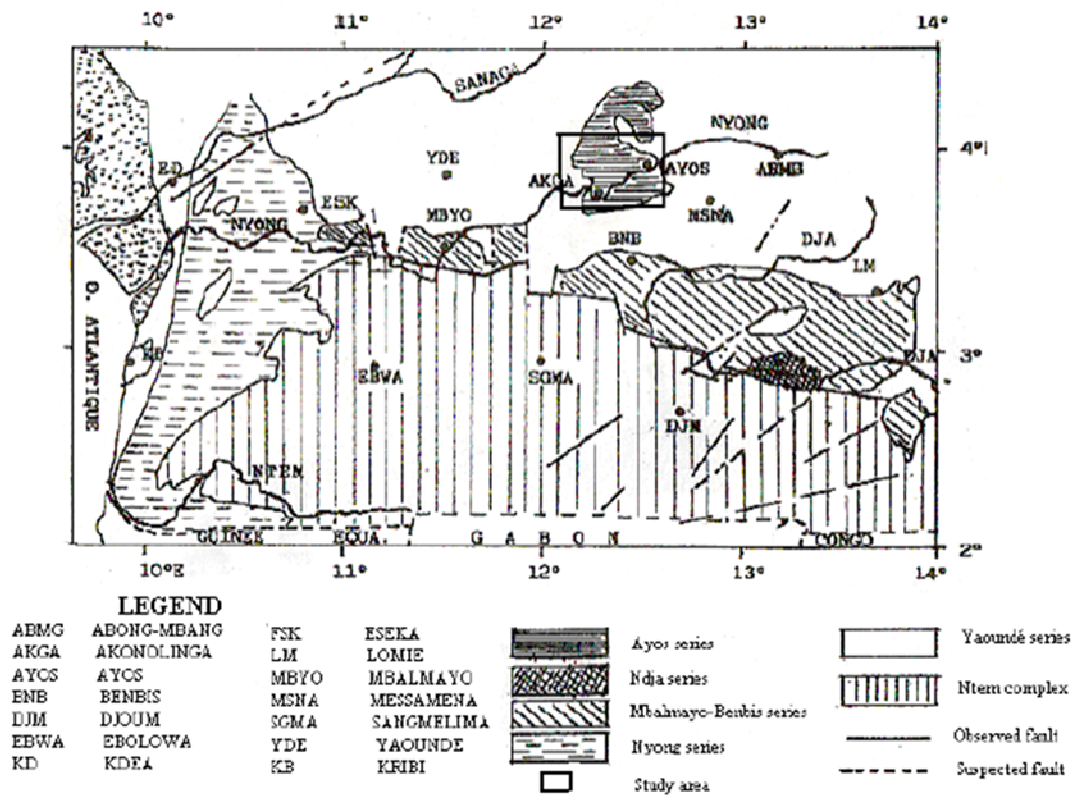


Figure 1a. Simplified major structural formation map of Southern Cameroon.

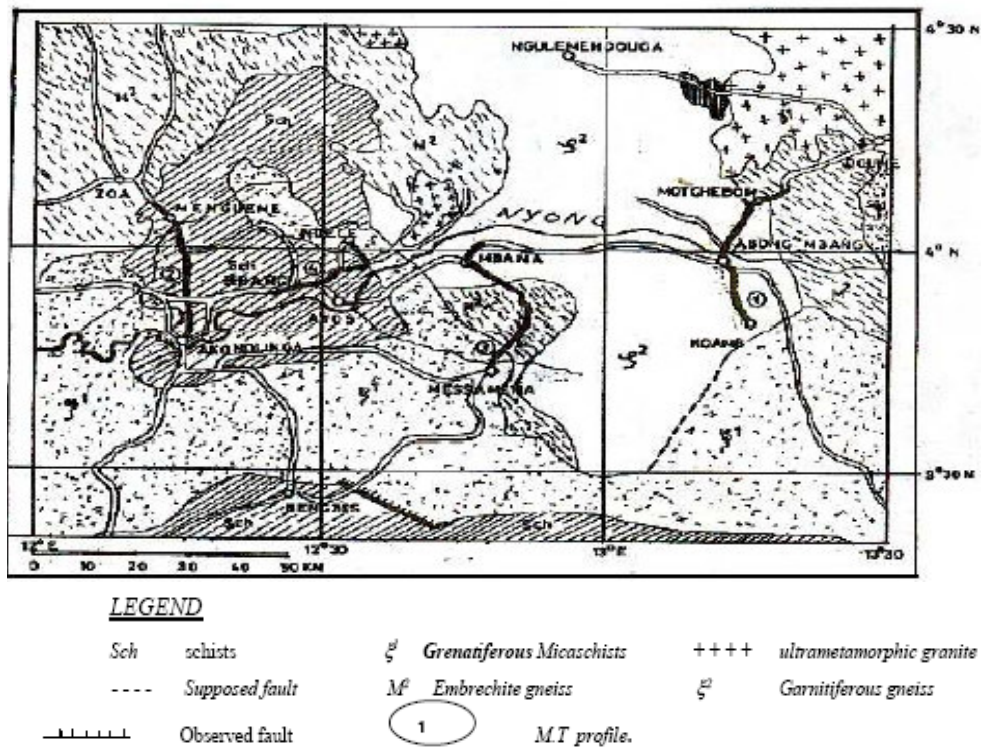


Figure 1b. Geological map of the area of study.

where  $\rho$  is the resistivity and  $T(s)$  is the period.

For tabular subsoil, the resistivity varies only with the period  $T$ .  $\rho$  given by (1) is an apparent resistivity  $\rho_a$  (Pham-Vam et al., 1978) and (1) becomes (2) as follows:

$$\rho_a = 0.2T \left| \frac{E_x}{H_y} \right|^2 \tag{2}$$

The penetration depth is the depth corresponding to the amplitude of the wave such that it is reduced by 1/e that is to say about 37% compared to the amplitude on the surface. This depth is given by:

$$P \text{ (km)} = 0.503 \sqrt{\rho_a T} \tag{3} \quad \rho_a \text{ (}\Omega\cdot\text{m)}$$

Bostick (1977) draws the curve of the apparent resistivity versus the frequency. The asymptote of this curve for low frequencies for a model of subsurface made up of a uniform resistivity section on the top of a perfectly conducting substratum is given by the formula below:

$$\rho_a = \omega \mu_0 h^2 \tag{4}$$

Where  $\omega = 2\pi f$  ( $f$  is the frequency),  $h$  is the depth and  $\mu_0$  is the magnetic permeability.

For a soil model made up of the same resistive section, with the top of a substratum perfectly insulated and of infinite thickness, the equation of this asymptote is given by:

$$\rho_a = \frac{1}{\omega \mu_0 s^2} \tag{5}$$

Where 
$$s = \int_0^h \sigma(z) dz$$

Combining equations (4) and (5) above, we obtain the expression of the Bostick transformation as shown below:

$$\rho(h) = \rho_a \frac{1 - m}{1 + m} \tag{6}$$

$$m = \frac{d \log \rho_a}{d \log f} = \frac{f}{\rho_a} \frac{d \rho_a}{df} \tag{7}$$

$m$  is the apparent resistivity gradient on the bilogarithmic scale. There is equivalence between the Bostick transformation and the Niblett approximation (Jones, 1983) which is resumed by the equation:

$$\sigma_N(h) = h \frac{d \sigma_a(T)}{dh} + \sigma_a(T) \tag{8}$$

Where  $\sigma_a$  is the apparent conductivity which varies with the depth,  $h$ .

**Equipment**

The apparatus used for measurement is a resistivimeter ECA 540-0. This resistivimeter ECA 540-0 is a scalar type composed of two identical selective measuring outlets, associated to an acquisition and calculation system that uses a microprocessor. At each station of measurement, the apparent resistivities are measured for twelve audio frequencies (4.1, 7.3, 13, 23, 41, 73, 130, 230, 410, 730, 1300 and 2300 Hz) and along two perpendicular directions. When we do not have information on the geology of the area, the rotation method of sounding (Manguelle-Dicoum et al., 1992) is a better means of determining the principal directions of the structures.

The data collected have been interpreted using several representations based on the Bostick (1977) and the classical (Cagniard, 1953; Vozoff, 1972, 1990) approaches. The Bostick resistivities are derived from the determination of the gradient of the slopes of resistivity curves. The differentiation of two geological units is possible through the pseudo-sections on which discontinuity appear, with a strong lateral gradient of resistivity.

**Determination of principal structural trends**

Due to the fact that the AMT scalar instrument (ECA 540-0) used is not designed for such simultaneous measurements, it has to be preceded by the determination of principal directions using the rotation sounding approach. According to Manguelle-Dicoum et al. (1992), the apparent resistivity  $\rho_a$  is measured as a function of the orientation angle of the telluric line and the principal directions deduced as those corresponding to the maximum and minimum resistivities which are perpendicular to each other (Figures 2a and b). In this approach, the fundamental assumption is that, the directions of resistivities extrema coincide with the directions of the principal structural trends.

In the Akonolinga-Ayos area, to palliate to the fact that we used an AMT scalar instrument, we have applied the rotation sounding approach (Manguelle-Dicoum et al., 1992).

**PRESENTATION OF RESULTS**

**Description of the profiles**

**Profile 1: Akonolinga-Mengueme**

Profile1 (Figure 1c) is crossing parallel 4°N and comprises 9 stations of measurement (A<sub>1</sub>... A<sub>9</sub>). This profile directed S-N, crosses the Western part of the Ayos series and extends from Akonolinga to the North of Mengueme. The area of investigation is consequently located on quartzites dominating at the South and the Center and of schists at the North. Station A<sub>9</sub> is located near a geological contact, schist- embrechites gneiss of SW-NW direction, on the Western limit of the Ayos series (Mbom-Abane, 1997). Geological, it is attributed an E-W direction and a Northern dip to the metamorphic rocks of the central zone of the profile.

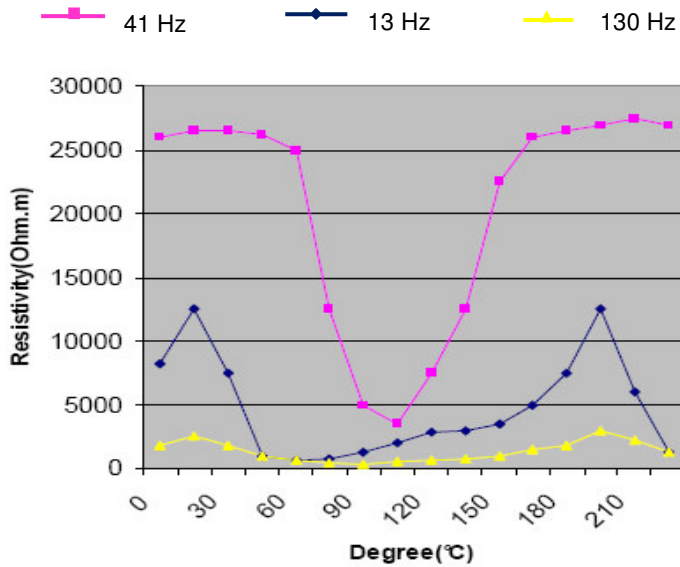


Figure 2a. Rotation soundings Akonolinga1.

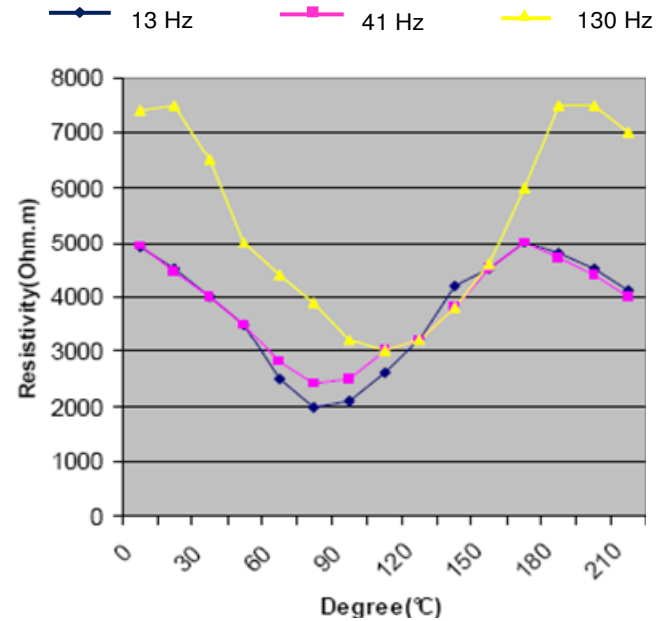


Figure 2b. Rotation soundings Ayos 2.

## Profile 2: Mbang-Metol

This profile (Figure 1c) also crosses parallel 4°N and has 9 stations, noted  $B_i$  ( $i = 1 \dots 9$ ). The stations from  $B_1$  to  $B_5$  are located on the schists of the Ayos series and the stations from  $B_6$  to  $B_9$  on the garnetiferous micaschists (Figure 1b). Station  $B_1$  is located on the Northern bank of the Nyong stream. Stations from  $B_6$  to  $B_8$  are near a schist-micaschists contact with direction N-NW, while station  $B_9$  is located to the South of the schists-micaschist contact.

## Results from the classical approach

### Profile 1: Apparent resistivity profiles and pseudo-section

The apparent resistivity profiles (Figures 3a - b) show that the subsoil is relatively homogeneous between the stations  $A_7$  and  $A_9$ . The pseudo-section (Figure 4a) shows two high resistive zones at greater depth; from  $A_1$  to  $A_2$  and from  $A_4$  to  $A_5$  respectively. These two resistive zones are separated by a conductive zone at station  $A_3$ . There is also a quasi homogeneous zone characterised by sub-horizontal iso-resistivities from  $A_7$  to  $A_9$ . Discontinuities are observed at stations  $A_3$  and  $A_6$  as shown by the pseudo-section and the apparent resistivity profiles. These discontinuities correspond to conductive anomalies.

### Geoelectrical section

The models obtained have four layers for stations  $A_1$ ,  $A_2$ ,

$A_3$ ,  $A_5$  and three layers for the other stations. The models with four layers have first and third layers being very conductive. The geoelectrical section presents two major zones of discontinuity between  $A_3$  and  $A_4$  and the second between  $A_6$  and  $A_7$  (Figure 4b) which correspond to a deep seated fault directed E-W.

The geoelectrical section of the direction of measurement N105°E in combination with the standard table of resistivity range for rocks (Parasnis, 1997) and the geological information (Figures 1a - b) have enabled us to propose a geological section of the subsurface (Figure 5).

### Profile 2: Apparent resistivity profiles and pseudo-section

The apparent resistivity profiles (Figures 6a - b) show two discontinuities at  $B_4$  and  $B_6$  respectively. The pseudo-section (Figure 7a) shows a resistive zone from  $B_1$  to  $B_5$  comprising a conductive zone at  $B_4$ ; a quasi homogeneous zone from  $B_7$  to  $B_9$  at medium and higher depths and a conductive zone which separates the resistive and the quasi homogeneous zones.

The pseudo-section also shows the same discontinuities as the apparent resistivity profiles at  $B_4$  and  $B_6$ .

### Geoelectrical section

The models obtained here have three layers for stations  $B_1$  and  $B_5$  and four layers for the other stations. Models with four layers have first and third layers very conductive. The

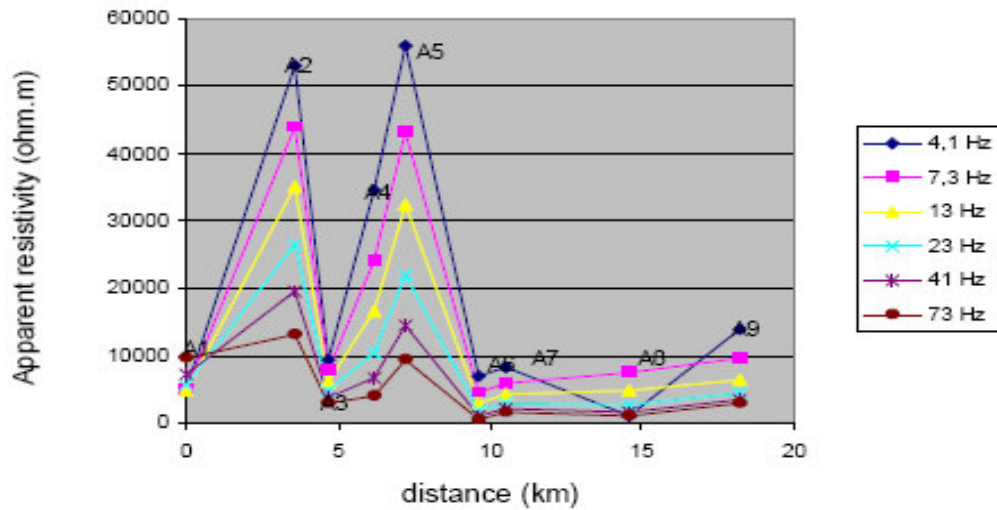


Figure 3a. Profiling curves for low frequencies (profile 1), classical approach.

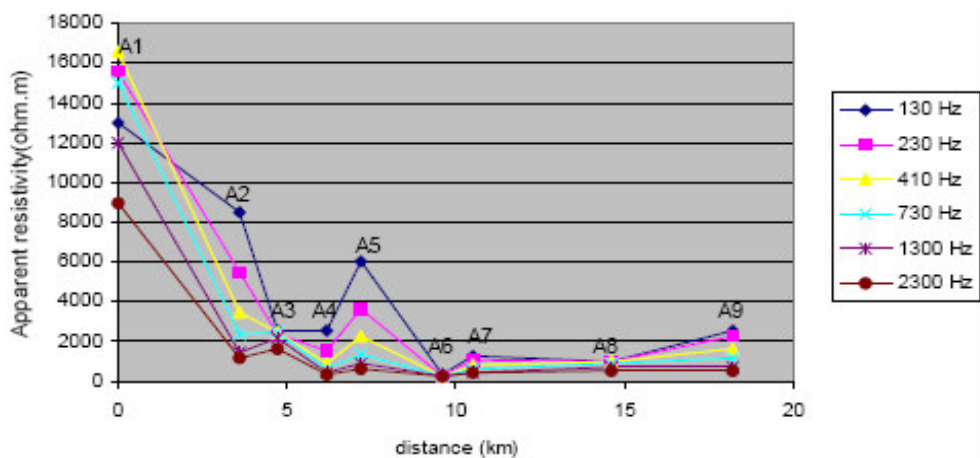


Figure 3b. Profiling curves for high frequencies (profile 1), classical approach.

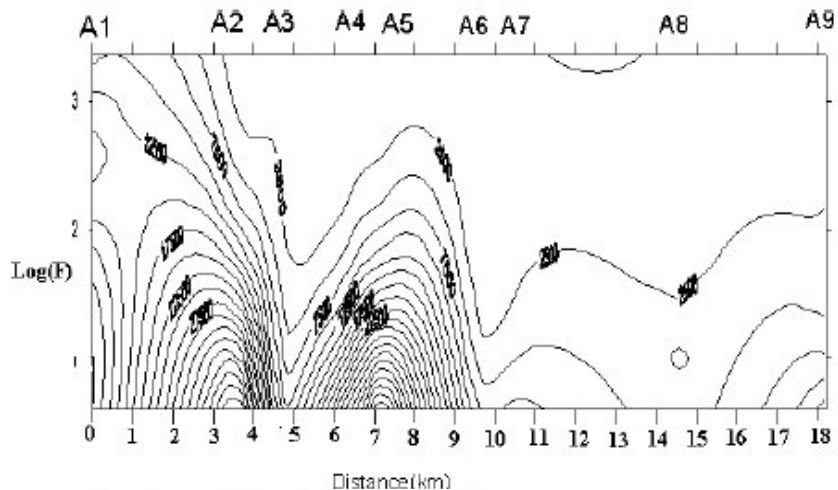


Figure 4a. Pseudo-section for profile 1, classical approach

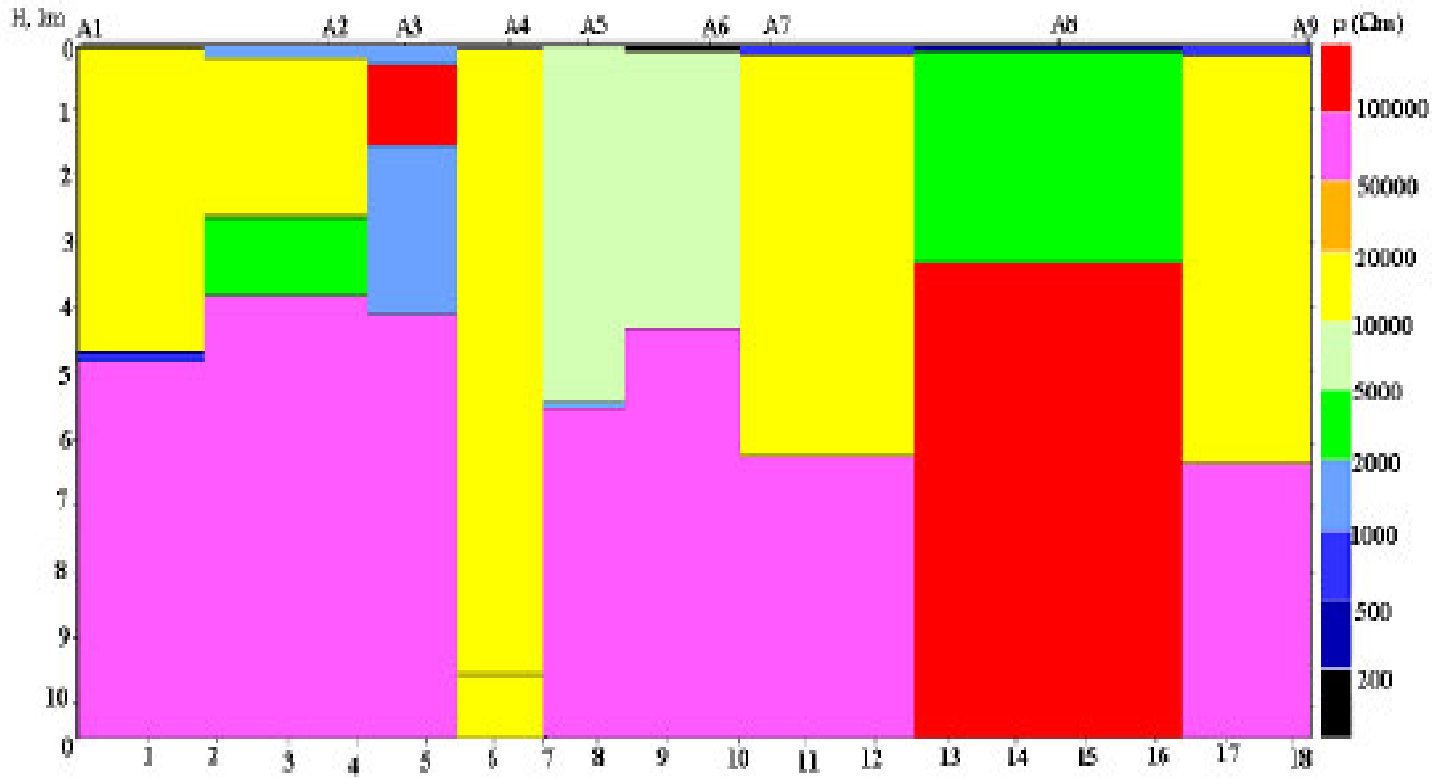


Figure 4b. Geoelectrical section of profile 1, classical approach.

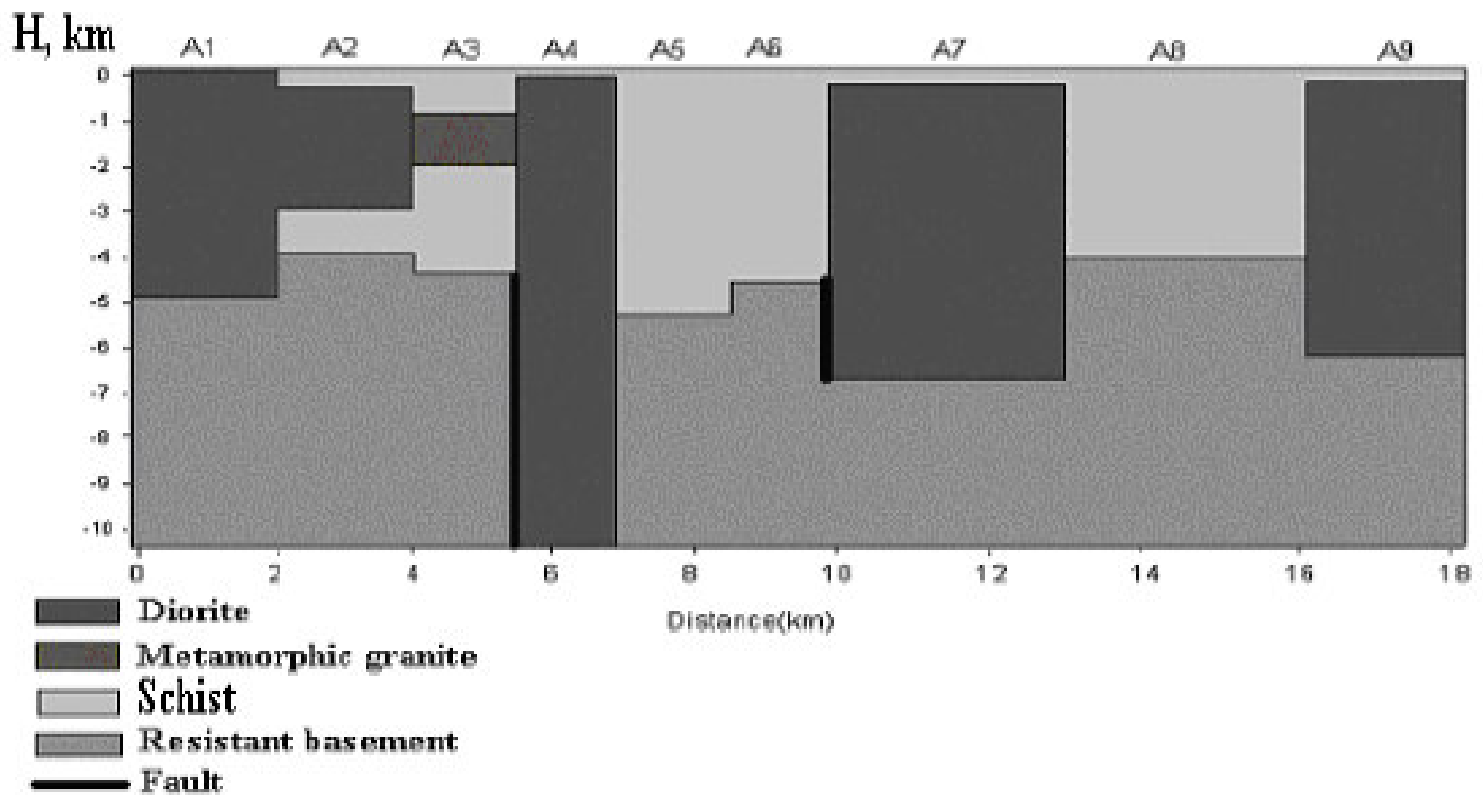


Figure 5. Geological section of profile 1, classical approach.

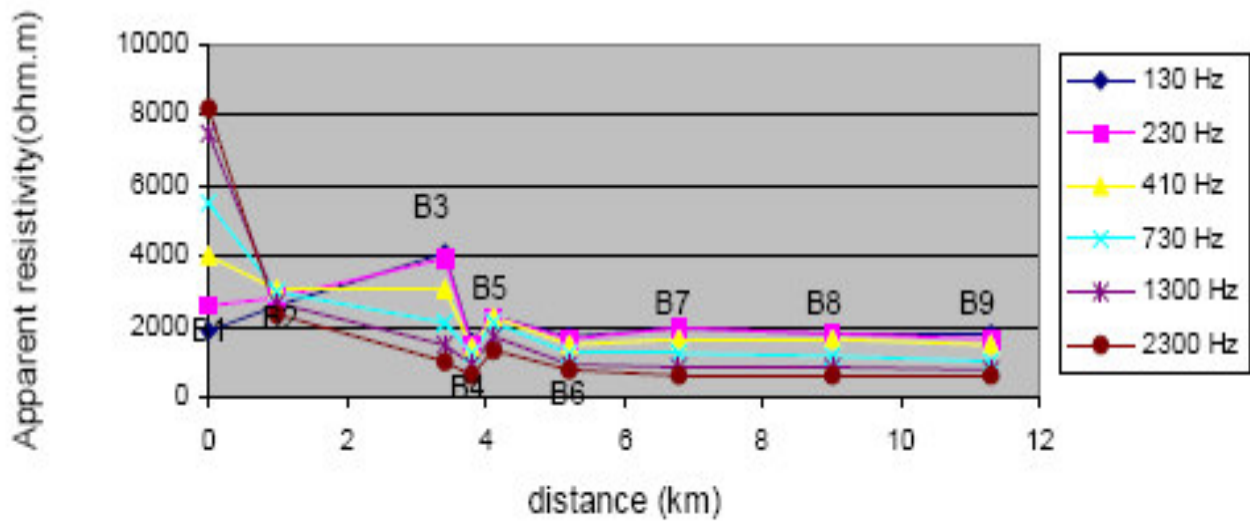


Figure 6a. Profiling curves for high frequencies (profile 2), classical approach,

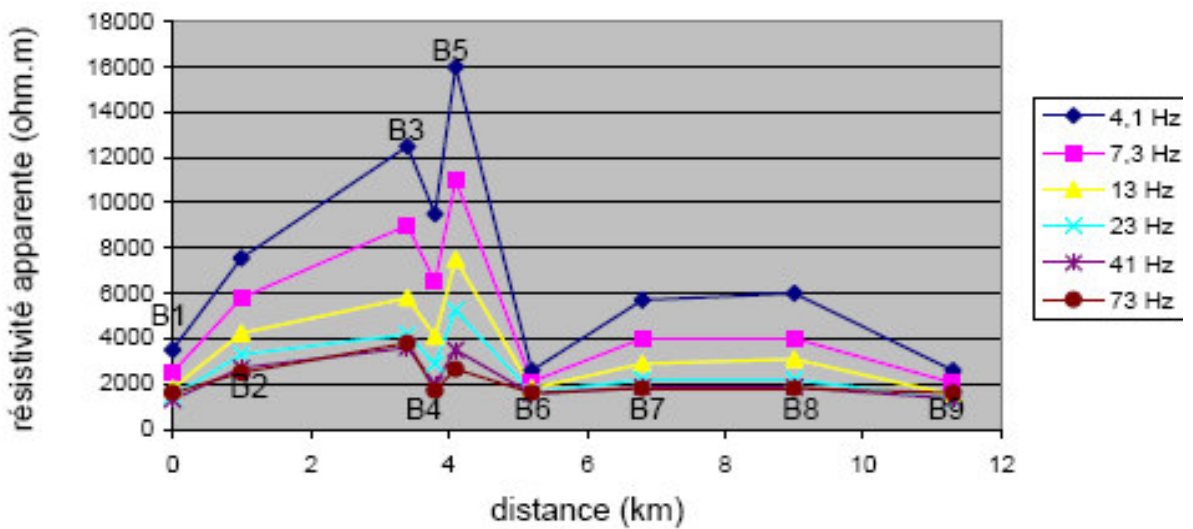


Figure 6b. Profiling curves for low frequencies (profile 2), classical approach,

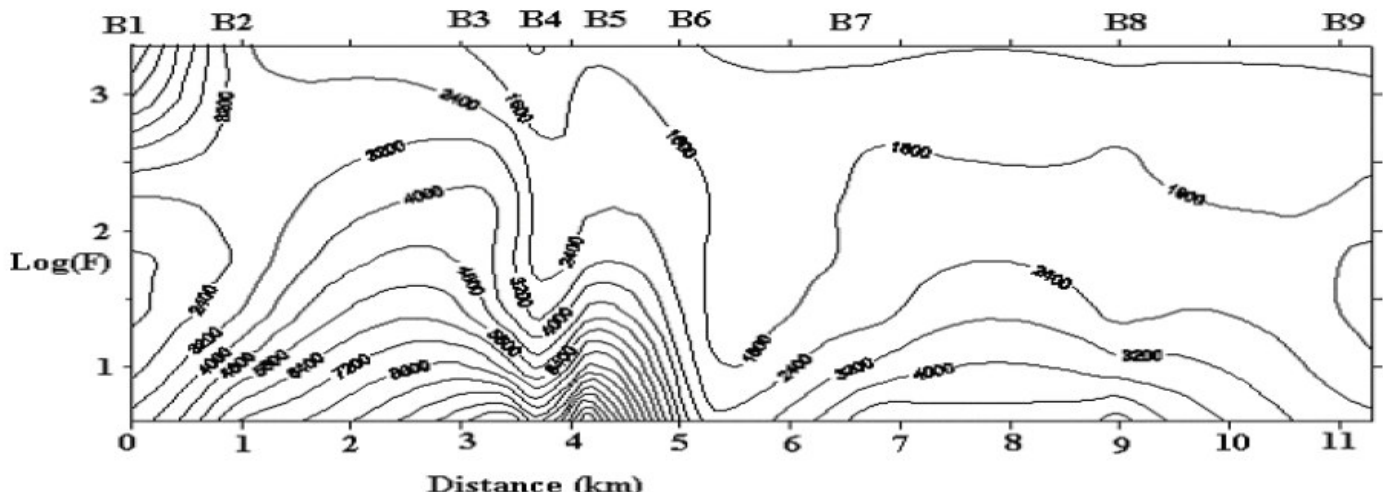


Figure 7a. Pseudo-section for profile 2, classical approach.

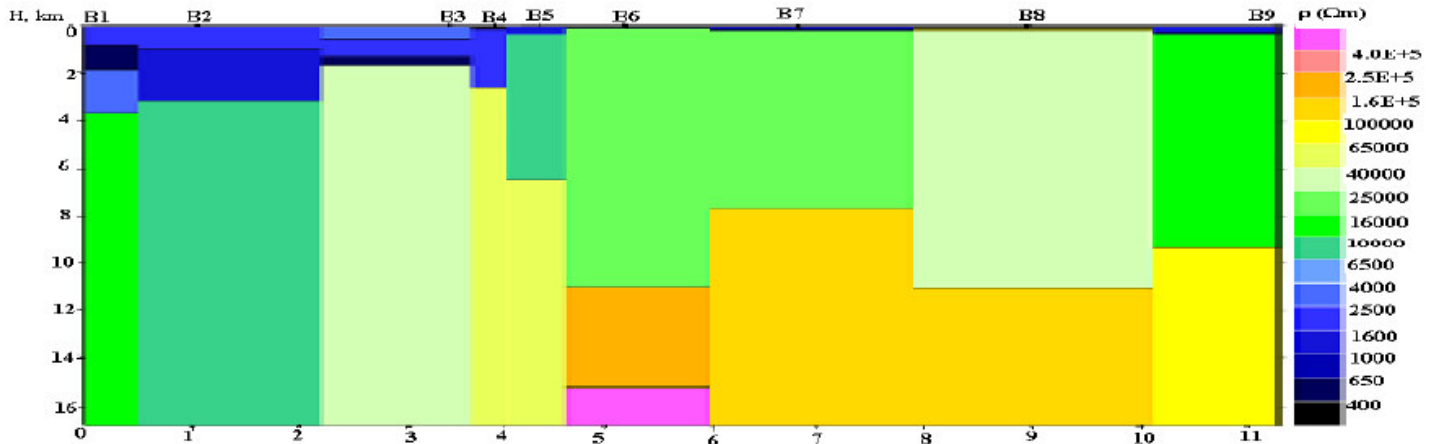


Figure 7b. Geoelectrical section of profile 2, classical approach.

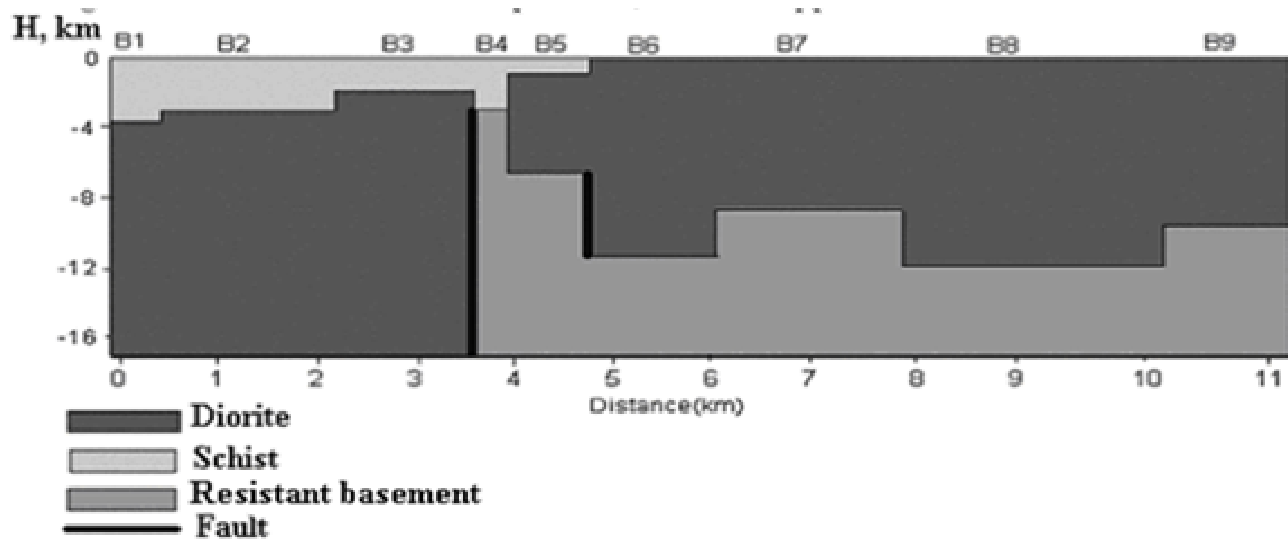


Figure 8. Geological section of profile 2, classical approach.

conductive. The geoelectrical (Figure 7b) section has two major zones of discontinuities at B<sub>4</sub> and B<sub>6</sub> which correspond to a deep seated fault directed E-W.

The geological section of the direction of measurement N75°E in combination with the standard table of resistivity range for rocks (Parasnis, 1997) and the geological information (Figures 1a - b) has helped us to deduce the geological section of the subsurface (Figure 8).

### Results from the Bostick approach

#### Profile 1: Determination of the Bostick resistivities and soil models

From the resistivity gradient vs. depth variations, one can

obtain the number of slopes for each curve in the two directions of measurement. The determinations of the values of these different slopes make it possible to deduce the Bostick resistivities from formula (6). The Bostick resistivity corresponds to the resistivity of a layer whose thickness is deduced from the resistivity gradient vs. depth curve (Bostick, 1977). For each station, we can therefore obtain directly the model of the corresponding soil. This model does not emphasize the last layer which generally has an infinite depth.

#### The pseudo-section and the Geoelectrical section

The pseudo-section (Figure 9a) shows several zones of discontinuity. These zones can be seen at A<sub>3</sub>, A<sub>6</sub> and

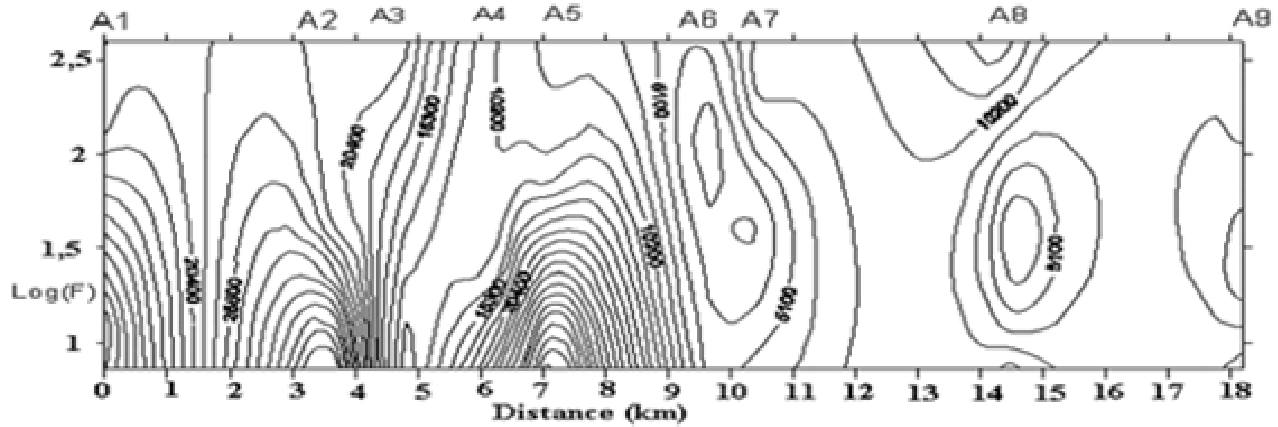


Figure 9a. Pseudo-section for profile 1, Bostick approach.

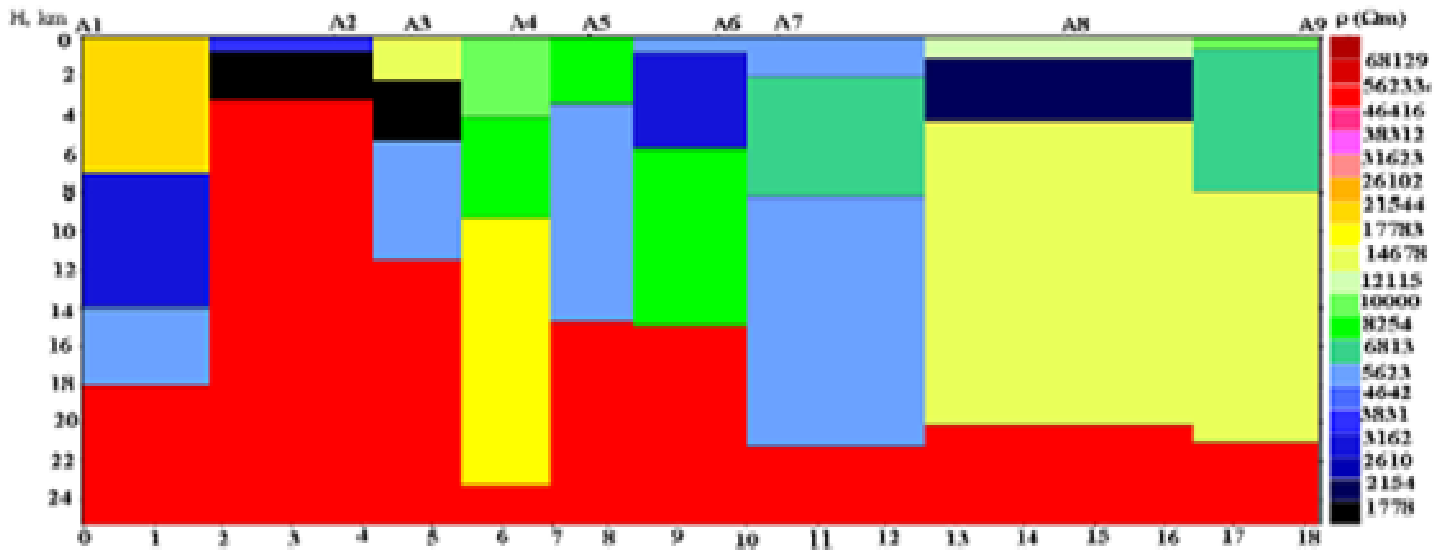


Figure 9b. Geoelectrical section of profile 1, Bostick approach.

A<sub>8</sub>. The results emerging from the study of the geoelectrical section (Figure 9b) show zones of discontinuity between A<sub>3</sub> and A<sub>4</sub> and A<sub>6</sub> and A<sub>7</sub>. On the other hand in the direction N105°E, we have a species of crushing structures between stations A<sub>4</sub> and A<sub>9</sub>. In the classical approach, this anomaly is characterized by a fault. Fractures have been observed between stations A<sub>8</sub> and A<sub>9</sub> in the direction N15°E and on the other hand between stations A<sub>4</sub> and A<sub>7</sub> in the N105°E direction. These fractures can be related to the tectonics of the area. The area of study indeed, is characterized by traces of ductile or breakable structures. The geoelectrical section in combination with the standard table of resistivity range for rocks (Parasnis, 1997) and the geological information (Figures 1a - b) have led to the proposition of a geological section (Figure 10).

**Profile 2**

To obtain the Bostick resistivities and the subsurface model of the area of study, we proceed like in profile 1 above. The pseudo-section between B<sub>1</sub> and B<sub>2</sub> (Figure 11a) shows closed iso-resistivities which are almost vertical, but in a whole does not provide enough details that can permit the characterisation of the area under study. The analysis of the geoelectrical section (Figure 11b) shows between B<sub>3</sub> and B<sub>6</sub> a species of crushing structures and a fracture between B<sub>8</sub> and B<sub>9</sub> in direction N165°E. In the direction N75°E, there is a discontinuity between B<sub>3</sub> and B<sub>5</sub>. The geological section (Figure 12) of the subsurface model has been brought to evidence through the combination of the geoelectrical section with the standard table of resistivity range for rocks (Parasnis,

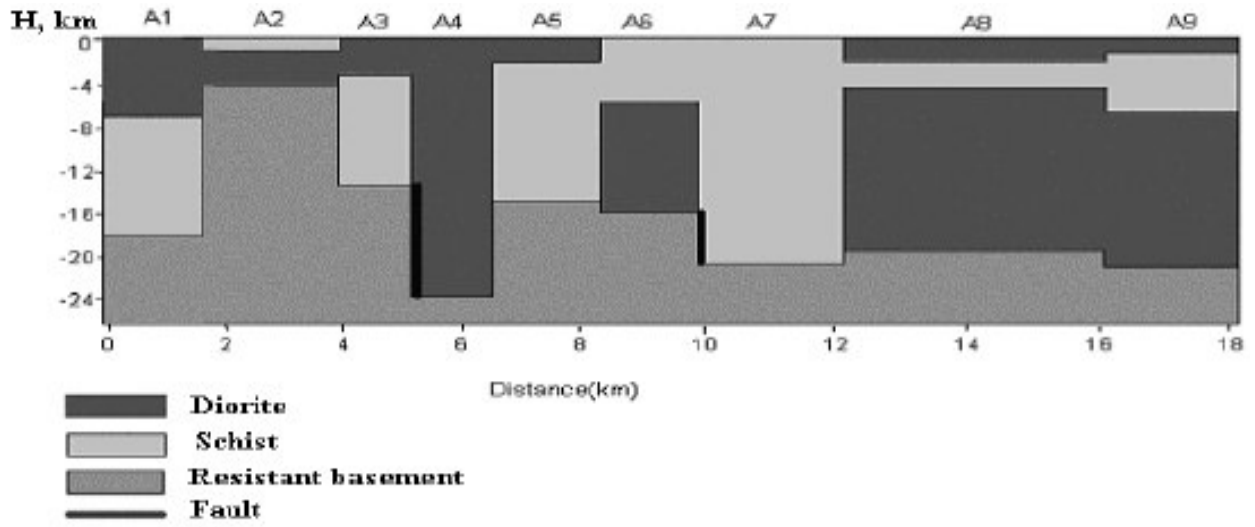


Figure 10. Geological section of profile 1, Bostick approach.

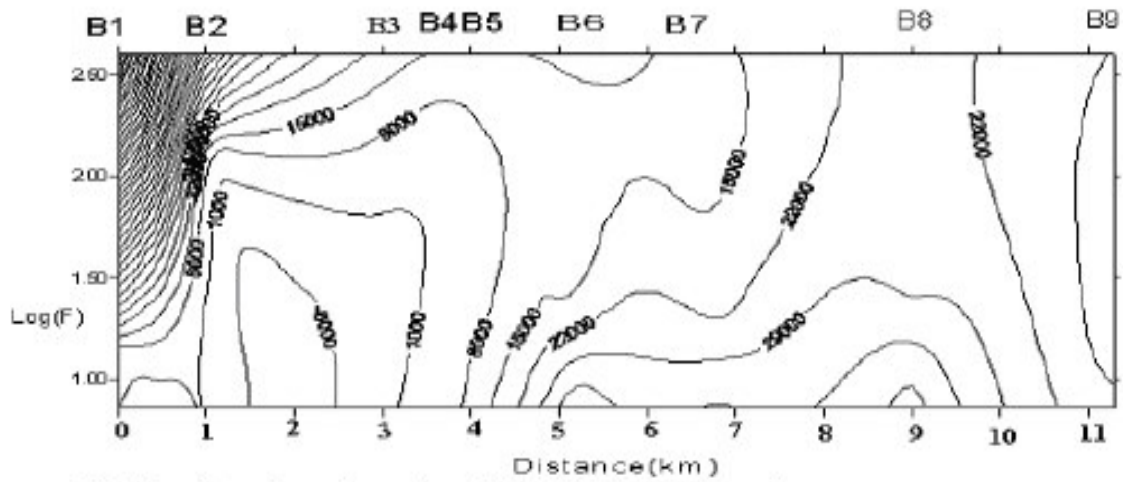


Figure 11a. Pseudo-section for profile 2, Bostick approach.

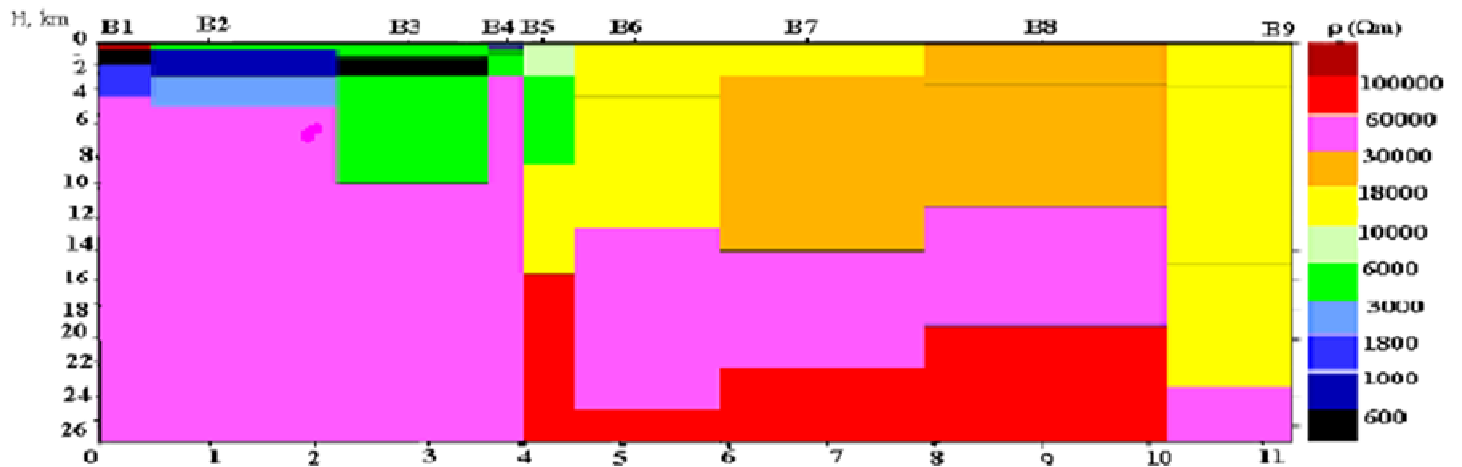


Figure 11b. Geoelectrical section of profile 2, Bostick approach.

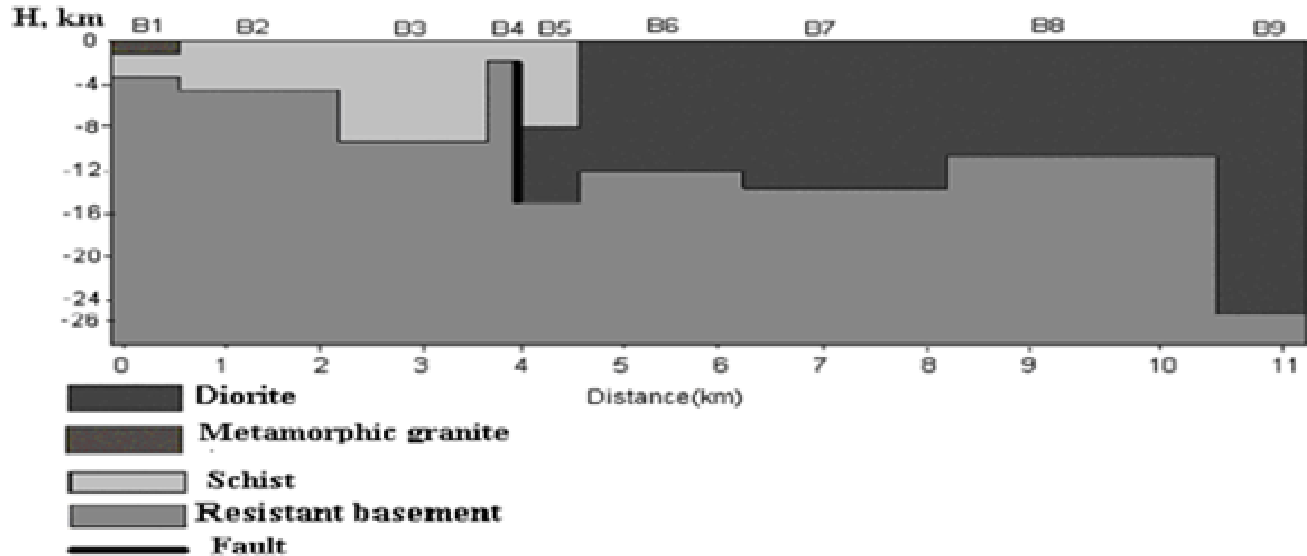


Figure 12. Geological section of profile 2, Bostick approach.

1997) and the geological information of the area of study (Figures 1a and b).

## DISCUSSION

The resistivity profiles reveal two zones of discontinuity; between  $A_2$  and  $A_3$ ,  $A_5$  and  $A_6$  for profile 1 and at  $B_4$  and  $B_6$  for profile 2. The analysis of the pseudo-sections for the two approaches has shown that the anomaly at  $A_3$  would be characteristic of a fault.

The study of the pseudo-section for profile 1, through the Bostick approach shows more details of the zone of investigation but does not provide enough information for profile 2 as iso-resistivities are tightened between stations  $B_1$  and  $B_2$ . We observe that, the geoelectrical sections of the two profiles have similarities in the number of layers and forms presented.

The study of the geoelectrical section for profile 1, through the classical approach reveals a major fracture between  $A_3$  and  $A_4$  meanwhile, the Bostick approach reveals a species of crushing structures between  $A_4$  and  $A_9$  in addition to the major fracture identified between  $A_3$  and  $A_4$ . As concerns profile 2, the geoelectrical section of the classical approach reveals discontinuities between  $B_3$  and  $B_4$  and also shows simple contacts between different layers. This Bostick approach also reveals a discontinuity between  $B_3$  and  $B_5$ . The analysis of the geoelectrical sections of the two profiles show that the Bostick approach provides information of greater depth.

The combination of classical and Bostick approaches has led to the revelation of a major fracture identified as a fault, oriented E-W, hidden by cover formations and a crushing structural system. These findings are in correlation with geological observations (Olinga et al.,

2009). The results obtained are in accordance with a gravity study carried out by Ndougsa-Mbarga et al. (2003) along the parallel 4°N which showed a normal fault oriented E-W in the Mengueme-Akonolinga area. This study also revealed a major contact of rocks between the schist-quartzite complex and the charnokite-granulitic group (Ndougsa et al., 2003). The species of crushing structures result from the tectonics napes having moderated their dip with a southern vergency (Vignès-Adler et al., 1991; Penaye et al., 1993; Olinga et al., 2009) derived from the overlapping of the Central African Mobile Zone (CAMZ) on the Congo Craton (CC).

## Conclusion

A geophysical investigation from the combination of the classical and Bostick approaches has significantly contributed to the understanding of the underground structure of the Akonolinga-Ayos zone. This zone is indeed, characterized by a species of crushing structures between Ebale and Envong along profile 1 and between Olembe and Awo'o along profile 2. This study has highlighted the presence of faults at Ngulntangan and Olembe. The Bostick approach has revealed the presence of metamorphosed granite lined between Mbang and Bil. The geological models of the subsoil suggested along these two profiles, although made up of probable structures, are initial models for future investigations.

The discussion resulting from the two approaches has enabled us to realize that the Bostick approach provides more detailed information than the classical approach in certain representations. The principal conclusion which arises from this study is that, for a good interpretation of AMT data, we must associate the two methods because

their results are complementary.

## REFERENCES

- Bostick FX (1977). A simple almost exact method of MT analysis. Workshop on Electrical Methods in Geothermal Exploration, U.S. Geol. Surv., Contract No. 1408000-8-359. p. 10
- Cagniard L (1953). Basic theory of the magneto telluric method of geophysical prospecting. *Geophys.*, 18: 605-635.
- Jones AG (1983). On the Equivalence of the Niblett and Bostick transformation in the Magneto telluric Method. *Geophys.*, 53: 72-73.
- Manguelle-Dicoum E, Bokossah AS, Kwende-Mbanwi TE (1992). Geophysical evidence for a major Precambrian schist-granite boundary in Southern Cameroon. *Tectonophys.*, 205: 437-446.
- Mbom-Abane S (1997). Investigation géophysique en bordure du Craton du Congo (région d'Abong – Mbang / Akonolinga – Cameroun) et implications structurales. Thèse Doctorat d'Etat ès Sciences, Univ. de Yaoundé I, Fac. Sciences. p.187.
- Ndougsa-Mbarga T, Manguelle-Dicoum E, Tabod CT, Mbom-Abane S (2003). Modélisation d'anomalies gravimétriques dans la région de Mengueme-Akonolinga (Cameroun). *Sci. Technol. Dev.*, 10(1): 67-74.
- Niblett ER and Sayn-Wittgenstein C (1960). Variation of electrical conductivity with depth by the magneto telluric method. *Geophys.* 25: 998-1008.
- Nzenti JP, Barbey P, Macaudiere J, Soba D (1988). Origin and Evolution of the Precambrian high grade Yaoundé gneiss (Cameroun). *Precambrian Res.*, 38: 91-109.
- Olinga JB, Mpesse PM, Minyem D, Ngako V, Ndougsa Mbarga T, Ekodeck G (2009). The Awaé-Ayos strike-slip shear zones (southern Cameroon): Geometry, kinematics and significance in the late Pan-African tectonics. Accepted for publication in *Neues Jahrbuch für Geologie und Paläontologie*.
- Parasnis DS (1997). Principles of Applied Geophysics: 5th edition Chapman and Hall, London, England p. 400.
- Penaye J, Toteu SF, Van Schmus WR, Nzenti JP (1993). U-Pb and Sm-Nd preliminary geochronologic data on the Yaoundé Series, Cameroun: re-interpretation of the granulitic rocks as the suture of collision in the Central African Belt. *C.R. Acad. Sci., Paris*, 317(2):789-794.
- Pham VN, Boyer D, Chouteau M (1978). Mapping of apparent pseudoresistivity by combination of Telluric-Telluric and magnetotelluric profiling. *Geophys. Prospect.*, 26: 218-246.
- Ritz M (1982). Etude régionale M.T. des structures de la conductivité électrique sur la bordure occidentale du Craton Ouest Africain en République du SENEGAL. *Can. J. Earth Sci.*, 19 : 1408-1416.
- Rolin P (1995). La zone de décrochement panafricain des OUBANGUIDES en République Centrafricaine. *C.R. Acad. Sci.*, 320(2A) : 63-69.
- Toteu SF, Penaye J, Poudjom-Djomani Y (2004). Geodynamic evolution of the Pan-African with special reference to Cameroon. *Can. J. Earth Sci.*, 41:73-85.
- Vignes-Adler M, Le Page A, Adler PM (1991). Fractal analysis of fracturing in two African regions from satellite imagery to ground scale. *Tectonophys.*, 16: 69-86.
- Vozoff K (1972). The Magnetotellurics method in the exploration of sedimentary basins. *Geophys.*, 37(1): 98-141.
- Vozoff K (1990). Magnetotelluric principles and practice. *Proc. Indian Acad. Sci. (Earth Sci.)*, 99(4): 441-471.